The Journal of Immunology

SLAT Regulates CD8$^+$ T Cell Clonal Expansion in a Cdc42- and NFAT1-Dependent Manner

Sonia Feau, Stephen P. Schoenberger, Amnon Altman and Stéphane Bécart

J Immunol 2013; 190:174-183; Prepublished online 28 November 2012;
doi: 10.4049/jimmunol.1201685
http://www.jimmunol.org/content/190/1/174

The Journal of Immunology is published twice each month by
The American Association of Immunologists, Inc.,
1451 Rockville Pike, Suite 650, Rockville, MD 20852

Print ISSN: 0022-1767 Online ISSN: 1550-6606.

SLAT Regulates CD8$^+$ T Cell Clonal Expansion in a Cdc42- and NFAT1-Dependent Manner

Sonia Feau,* Stephen P. Schoenberger,* Amnon Altman,[†,1] and Stéphane Bécart[†,1]

After antigenic stimulation, CD8$^+$ T cells undergo clonal expansion and differentiation into CTLs that can mount a strong defense against intracellular pathogens and tumors. SWAP-70–like adapter of T cells (SLAT), also known as Def6, is a novel guanine nucleotide exchange factor for the Cdc42 GTPase and plays a role in CD4$^+$ T cell activation and Th cell differentiation by controlling Ca^{2+}/NFAT signaling, but its requirement in CD8$^+$ T cell response has not been explored. Using a range of transgenic and knockout in vivo systems, we show that SLAT is required for efficient expansion of CD8$^+$ T cells during the primary response but is not necessary for CTL differentiation. The reduced clonal expansion observed in the absence of SLAT resulted from a CD8$^+$ T cell–intrinsic proliferation defect and a reduced IL-2–dependent cell survival. On a molecular level, we show that *Def6* deficiency resulted in defective TCR/CD28-induced NFAT translocation to the nucleus in CD8$^+$ T cells. Constitutively active Cdc42 or NFAT1 mutants fully restored the impaired expansion of *Def6*$^{-/-}$ CD8$^+$ T cells. Taken together, these data describe a new and pivotal role of SLAT-mediated NFAT activation in CD8$^+$ T cells, providing new insight into the signaling pathways involved in CD8$^+$ T cell proliferation. *The Journal of Immunology*, **2013, 190: 174–183.**

A functional CD8$^+$ T cell response is critical for host defense against intracellular pathogens and malignancies. Upon recognition of cognate Ag, naive CD8$^+$ T cells undergo a vigorous Ag-specific clonal expansion and differentiation into effector CD8$^+$ CTLs, producing cytokines (mainly IFN-γ and TNF-α) and cytotoxic effector molecules (such as perforin and granzyme B) to mediate direct killing of target cells. Once an infection has been successfully cleared, the CTLs undergo a rapid contraction phase characterized by extensive cell death of the majority (>90%), leaving behind a stable pool of long-lived memory cells that provide long-term immunity against subsequent infections via rapid reactivation (1). It has been shown that extracellular stimuli such as Ag, costimulatory molecules (2, 3), and cytokines (4, 5) instruct naive CD8$^+$ T cells for clonal expansion and memory formation. The integration of these instruction signals triggers downstream intracellular signaling pathways leading to specific transcriptional programs that govern the fate of CD8$^+$ T cells (i.e., activation, proliferation, survival, differentiation). This research area remains intensively studied and is crucial for the design of novel vaccines against malignancies and pathogen infections.

SWAP-70–like adapter of T cells (SLAT; also known as IBP or Def6), which is encoded by the *Def6* gene, has been recently identified as a novel TCR-regulated guanine nucleotide exchange factor (GEF) for Cdc42 (and to a lesser extent Rac1) (6–8). SLAT is abundantly expressed in central and peripheral lymphoid tissues, with high levels found in thymocytes and peripheral T cells (7, 9, 10). Our previous examination of *Def6*-deficient (*Def6*$^{-/-}$) mice revealed SLAT to be a critical selective regulator of the TCR-coupled Ca^{2+}/NFAT signaling pathway (10), controlling positively CD4$^+$ Th cell activation and differentiation, as evidenced by its critical role in the development of T cell–dependent inflammatory diseases such as asthma (10) or experimental autoimmune encephalomyelitis (11). Moreover, the Ca^{2+}/NFAT regulatory activity of SLAT depends on actin polymerization and functional Cdc42 activity (6). Although the function of NFAT in CD4$^+$ T cell activation and differentiation is well established, its role in CD8$^+$ T cells is less clearly defined. Although NFAT transcriptional activity seems to be limited in Ag-stimulated CD8$^+$ T cells by comparison with CD4$^+$ T cells (12), NFAT1 has been shown to translocate to the nucleus of CD8$^+$ T cells upon TCR stimulation and to regulate IFN-γ gene expression (13). In addition, NFAT1 and its Ca^{2+}/calmodulin-dependent phosphatase, calcineurin, have been implicated in peripheral CD8 tolerance in vivo (14). Finally, silencing of cytokine production by CD8$^+$ T cells during chronic viral infections, such as murine lymphocytic choriomeningitis virus and human HIV, has been causally linked to impaired NFAT nuclear translocation (15).

In this study, we examined the involvement of SLAT in CD8$^+$ T cell activation and differentiation in vivo. We found that SLAT was required for the expansion of Ag-specific CD8$^+$ T cells during the primary response by intrinsically promoting their proliferation and by regulating the rate of CD8$^+$ T cell survival in an IL-2–dependent manner. In contrast, SLAT was not critical for CD8$^+$ T cell effector functions, such as cytokine production, degranulation, and cytolytic activity. Furthermore, constitutively active Cdc42 or NFAT1 mutants restored the proliferation of *Def6*$^{-/-}$ CD8$^+$ T cells in vivo. These data highlight a new role of SLAT and

*Division of Developmental Immunology, La Jolla Institute for Allergy and Immunology, La Jolla, CA 92037; and [†]Division of Cell Biology, La Jolla Institute for Allergy and Immunology, La Jolla, CA 92037

[1]A.A. and S.B. share senior authorship.

Received for publication June 19, 2012. Accepted for publication October 26, 2012.

This work was supported by National Institutes of Health Grants AI068320 (to A.A.) and AI076972 (to S.P.S.), the Kurz Family Foundation (to S.P.S.), and fellowships from the Diabetes & Immune Disease National Research Institute (to S.B.) and the Philippe Foundation (to S.B.). This is manuscript number 1507 from the La Jolla Institute for Allergy and Immunology.

Address correspondence and reprint requests to Dr. Stéphane Bécart, La Jolla Institute for Allergy and Immunology, 9420 Athena Circle, La Jolla, CA 92037. E-mail address: sbecart@liai.org

The online version of this article contains supplemental material.

Abbreviations used in this article: B6, C57BL/6J; BM, bone marrow; DC, dendritic cell; Eomes, Eomesodermin; β-Gal, β-galactosidase; GEF, guanine nucleotide exchange factor; ICS, intracellular cytokine staining; IS, immunological synapse; Lm-OVA, OVA-expressing *Listeria monocytogenes*; MPEC, memory precursor effector cell; SLAT, SWAP-70–like adapter of T cells; SLEC, short-lived effector cell; SLO, secondary lymphoid organ; Tg, transgenic; WT, wild-type.

www.jimmunol.org/cgi/doi/10.4049/jimmunol.1201685

its proximal (Cdc42) and distal (NFAT) effectors in $CD8^+$ T cell biology. Thus, SLAT may represent a novel target for manipulating $CD8^+$ T cell expansion in vaccination and other immunotherapies.

Materials and Methods

Mice

Mice were maintained under specific pathogen–free conditions in accordance with guidelines of the Association for Assessment and Accreditation of Laboratory Animal Care International. The studies described in this article conform to the principles outlined by the Animal Welfare Act and the National Institutes of Health guidelines for the care and use of animals in biomedical research. C57BL/6J (B6; $CD45.2^+$), B6.SJL ($CD45.1^+$), and *Rag1*$^{-/-}$ mice were purchased from The Jackson Laboratory. B6 ($CD45.1/2^+$) mice were generated by crossing B6 ($CD45.2^+$) with B6.SJL ($CD45.1^+$) mice. *Def6*$^{-/-}$ mice on a B6 background (10), OVA-specific OT-I TCR-transgenic (Tg) $CD45.1^+$ and Act-mOVA/$K^{b-/-}$ mice on a B6 background (16) have been previously described. *Def6*$^{-/-}$ OT-I TCR-Tg $CD45.2^+$ mice were generated by crossing *Def6*$^{-/-}$ mice with OT-I TCR-Tg $CD45.2^+$ mice, and their T cells were used as a source of $V\beta5V\alpha2$ $CD8^+$ T cells specific for amino acid residues 257–264 of OVA ($OVA_{257–264}$; SIINFEKL peptide). Six- to twelve-week-old mice were used in all experiments.

Immunizations and adoptive transfers

Groups of mice were primed either with 5×10^6 Act-mOVA/$K^{b-/-}$ splenocytes i.v. or with 3000 CFU OVA-expressing *Listeria monocytogenes* (Lm-OVA) i.v. The mice were rechallenged 7 d later with 1×10^7 ActA-deficient ($ActA^-$) Lm-OVA i.v. For adoptive cotransfer, *Def6*$^{-/-}$ (CD45.2) and wild-type (WT; CD45.1) OT-I TCR-Tg mice were bled, and the number of OT-I cells was determined by counting and FACS staining for $V\alpha2^+V\beta5^+$ cells. Fifty of each *Def6*$^{-/-}$ and WT OT-I $CD8^+$ T cells were injected i.v. per mouse into naive recipient mice 1 d prior to immunization.

Tetramer staining

Cells were stained for 10 min at room temperature with PE-conjugated $OVA_{257–264}$–H-2-K^b tetramer (BD Pharmingen), followed by staining with anti-CD8 (PE–TR), anti-CD62L (Alexa Fluor 750), anti-CD44 (Alexa Fluor 700), anti-CD127 (allophycocyanin), and anti–KLRG-1 (PE–Cy7) Abs. The Abs were purchased from BD Pharmingen, eBioscience, or BioLegend. Samples were acquired and analyzed as described earlier.

CD107a staining

Splenocytes (1×10^6 to 2×10^6) from immunized mice were plated in 96-well round-bottom plates in 200 μl of culture medium plus $OVA_{257–264}$ peptide (1 μg/ml) in the presence of GolgiPlug, GolgiStop (BD Biosciences), and CD107a Ab for 5 h at 37°C. Cells were stained with anti-CD8 (PE–TR), CD44 (Alexa Fluor 700), CD45.1 (Pacific blue), and CD45.2 (PerCP–Cy5.5) followed by fixation with Cytofix/Cytoperm (BD Biosciences) for 20 min at 4°C. Fixed cells were subjected to intracellular staining in Perm/Wash buffer (BD Biosciences) for 30 min at 4°C with anti-CD107a. Abs were purchased from BD Pharmingen, eBioscience, or BioLegend. Samples were acquired and analyzed as described.

In vitro CFSE, annexin V, and active caspase-3 analysis by flow cytometry

Cell division was analyzed by prelabeling purified $CD8^+$ T cells with 1 μM CFSE (Molecular Probes; Invitrogen) and stimulating them (0.5×10^6/ml) with plate-coated anti-CD3 and soluble anti-CD28 mAbs (5 and 2.5 μg/ml, respectively) for 72 h. CFSE dilution was measured by flow cytometry. For parallel analysis of apoptosis, cells were incubated with annexin V (allophycocyanin) for 15 min in annexin-binding buffer (10 mM HEPES, 140 mM NaCl, 2.5 mM $CaCl_2$, pH 7.4), washed, fixed and permeabilized, and stained with a PE-conjugated Ab against active caspase-3 (BD Pharmingen).

Ex vivo restimulation and intracellular cytokine staining

Cytokine production was assessed as previously described (17). Briefly, splenocytes (1×10^6 to 2×10^6) from immunized mice were plated in 96-well round-bottom plates in the case of Act-mOVA/$K^{b-/-}$ priming or in 96-well flat-bottom plates in the case of Lm-OVA priming in 200 μl of culture medium (IMDM; Invitrogen) supplemented with 8% FCS (Omega Scientific), 1% L-glutamine (Invitrogen), 100 μg/ml streptomycin, 100 U/ml penicillin, and 50 μM 2-mercaptoethanol (Sigma-Aldrich) plus $OVA_{257–264}$ peptide (1 μg/ml) in the presence of GolgiPlug (BD Biosciences) for 5 h at 37°C. Cells were stained with Abs against CD8 (PE–TR), CD62L (Alexa Fluor 750), CD44 (Alexa Fluor 700), CD45.1 (Pacific blue), and CD45.2 (PerCP–Cy5.5) followed by fixation with Cytofix/Cytoperm (BD Biosciences) for 20 min at 4°C. Fixed cells were subjected to intracellular cytokine staining (ICS) in Perm/Wash buffer (BD Biosciences) for 30 min at 4°C using anti-TNF (PE–Cy7), anti–IFN-γ (allophycocyanin), or anti–IL-2 (PE) Abs. Abs were purchased from BD Pharmingen, eBioscience, or BioLegend. The samples were acquired on an LSR II flow cytometer (Becton Dickinson), and data were analyzed with FlowJo software.

Ex vivo cytotoxicity assay

Def6$^{-/-}$ or WT OT-I mice were immunized i.v. with 5×10^6 Act-mOVA splenocytes. Activated ($CD44^{high}V\beta5^+$) OT-I $CD8^+$ splenocytes were sorted 7 d later. Different numbers of effector cells were seeded in quadruplicate in 96-well round-bottom plates in the presence of 1×10^5 Ova-expressing EL4 (mOVA-EL4) target cells, which were previously labeled for 6 h with [^{3}H]thymidine (2.5 μCi/ml) . Basal ^{3}H retention was determined by adding medium instead of effector cells. After overnight culture, cells were collected on glass-fiber filters, and the ^{3}H label retained in live target cells was measured in a β counter. The percentage of specific killing was calculated by the following formula: [(spontaneous cpm – experimental cpm)/spontaneous cpm] × 100.

In vivo proliferation assay

Def6$^{-/-}$ and WT OT-I splenocytes were isolated by negative selection (MACS; Miltenyi). WT $CD45.1^+CD90.2^+$ B6.SJL mice were injected (day −2) with CFSE-labeled 5×10^5 *Def6*$^{-/-}$ or WT OT-I cells (both expressing CD45.2) 1 d prior to being injected with 1×10^6 to 2×10^6 splenocytes from P14 lymphocytic choriomeningitis virus TCR-Tg $CD45.2^+$ $CD90.1^+$ mice, which served as an internal control. On day 0, mice were immunized with 5×10^6 Act-mOVA/$K^{b-/-}$ splenocytes i.v., and 3 d later spleens were harvested. Samples were acquired on an LSR II flow cytometer (Becton Dickinson), and data were analyzed with FlowJo software.

In vivo cytotoxic assay

Cytotoxicity assays were performed in immunized intact or in adoptively transferred mice. For intact mouse immunization, mice were primed with Act-mOVA/$K^{b-/-}$ splenocytes as described earlier. In the adoptive transfer system, B6 ($CD45.2^+$) mice were injected i.v. with 5×10^3 naive WT or *Def6*$^{-/-}$ ($CD45.1^+$) OT-I $CD8^+$ T cells. One day later (day 0), the mice were immunized i.v. with Act-mOVA/$K^{b-/-}$ splenocytes. Six days after immunization of intact mice or 5 d after immunization of adoptive transfer recipients, the mice received i.v. 5×10^6 B6.SJL ($CD45.1^+$) splenocytes, which were stained with 0.2 μM CFSE ($CFSE^{high}$) and loaded with the specific peptide ($OVA_{257–264}$) as a source of Ag-specific target cells. As a control, the mice also simultaneously received a similar number of splenocytes labeled with 0.02 μM CFSE ($CFSE^{low}$) and loaded with an irrelevant peptide (Ski9 peptide, $E1B_{192–200}$). Spleen cell suspensions were prepared 15 h later, and samples were acquired and analyzed as described earlier. Percent specific killing was calculated by the following formula: 100 − [(% $CFSE^{high}$/% $CFSE^{low}$ in primed condition)/(% $CFSE^{high}$/$CFSE^{low}$ in naive condition)].

Generation of retrogenic mice

The empty RV-IRES-GFP retroviral vector and a retroviral vector expressing a constitutively active Cdc42 ($Cdc42^{CA}$) mutant (pMX GFP Cdc42Q61L) have been described (18). The retroviral vector expressing a constitutively active form of NFAT1 containing two additional point mutations, which abolish NFAT homodimerization but not NFAT:AP-1 heterodimerization and, hence, leading to productive T cell activation (RV-CA-NFAT1-DCC′-QQEE or "$NFAT^{CA}$Δdimer"), was kindly provided by Dr. F. Macian (18). Platinum-E packaging cells (19) (0.5×10^6 cells) in 2 ml DMEM plus 10% FBS were plated in a 6-well plate. After overnight incubation, the cells were transfected with 3 μg retroviral plasmid DNA with TransIT-LT1 transfection reagent. After 24 h, the medium was replaced with complete DMEM containing 10% FBS. Cultures were maintained for 24 h, and the retroviral supernatant was harvested, filtered through 0.45-μm filters, and used for infection.

Bone marrow (BM) cells were harvested from the femurs of *Def6*$^{-/-}$ OT-I TCR-Tg $CD45.2^+$ or OT-I TCR-Tg $CD45.1^+$ mice. Lin^- cells were isolated by negative selection using a lineage cell depletion kit (MACS) and cultured in complete DMEM containing 20% FCS supplemented with IL-3 (10 ng/ml), IL-6 (20 ng/ml), and stem cell factor (50 ng/ml). After

24 h, the cells were resuspended in 0.5 ml complete DMEM and were added to 0.5 ml retroviral supernatant, supplemented with polybrene (5 μg/ml final concentration) and recombinant cytokines (IL-3, IL-6, and stem cell factor), and centrifuged at 2000 rpm for 1 h at room temperature. Cells were then incubated for 6 h at 32°C and cultured overnight at 37°C, followed by two additional retroviral infections at daily intervals. Transduced (GFP^+) progenitor cells were sorted and injected ($>2 \times 10^5$ cells) i.v. into sublethally irradiated (450 rad) recipient *Rag1*$^{-/-}$ B6 mice. Mice were analyzed 8 wk later for engraftment by analyzing their PBLs for $OVA_{257–264}$–H-2-K^b tetramer$^+$ $CD8^+$ T cells.

Subcellular fractionation and immunoblotting

Purified $CD8^+$ T cells (1×10^7) were washed with ice-cold PBS and resuspended in 100 μl buffer A (10 mM HEPES, pH 7.9, 10 mM KCl, 0.1 mM EDTA, 1 mM DTT, and proteases inhibitors) for 15 min on ice. Nonidet P-40 was then added to a final concentration of 0.5%, samples were quickly vortexed for 10 s and centrifuged for 2 min ($14{,}000 \times g$ at 4°C). The supernatant was collected as the cytosolic fraction. Nuclear pellets were washed twice with buffer A lacking Nonidet P-40, resuspended in 40 μl buffer B (20 mM HEPES, pH 7.9, 400 mM NaCl, 1 mM EDTA, 1 mM DTT, and proteases inhibitors), vortexed for 10 s, and rocked for 30 min at 4°C. Samples were centrifuged for 10 min at $14{,}000 \times g$, and the supernatant was collected as the nuclear fraction. Samples were resolved by SDS-PAGE, transferred to nitrocellulose membrane, and immunoblotted with Abs against hemagglutinin, lamin B, NFAT1 (4G6-G5) (both from Santa Cruz Biotechnology), β-actin (BioLegend), or rat α-tubulin (YL1/2; Serotec). Signals were detected using the ECL system (Amersham Biosciences).

Reporter assays

SV40 large T Ag-transfected human leukemic Jurkat T cells (Jurkat-TAg) were transfected with NFAT-luciferase plasmids plus a β-galactosidase (β-Gal) reporter plasmid as described (20). Transfected cells were cultured overnight, lysed, and luciferase or β-Gal activities were determined as described (20). The results are expressed in arbitrary luciferase units normalized to β-Gal activity in the same cells.

Statistical analysis

Data were analyzed using PRISM software (GraphPad, San Diego, CA). Differences between groups were examined for statistical significance using an unpaired two-tailed Student *t* test. Unless otherwise indicated, data represent the mean ± SEM, with $p < 0.05$ considered statistically significant.

Results

SLAT is critical for Ag-specific $CD8^+$ T cell primary expansion

Although SLAT is required for $CD4^+$ T cell activation and differentiation (6, 10, 11, 21), its role in $CD8^+$ T cells has not been addressed. To assess directly the in vivo requirement of SLAT in $CD8^+$ T cell responses, we immunized WT or *Def6*$^{-/-}$ mice with a nonreplicating, noninflammatory, cell-based immunogen (i.e., splenocytes from Act-mOVA mice), which expresses OVA under control of the actin promoter and has a homozygous deletion of the gene encoding H-2K^b (Act-mOVA/$K^{b-/-}$). These splenocytes cannot directly present the OVA Ag, leading to its cross-presentation by host APCs and, consequently, to cross-priming of functional H-2K^b–restricted $OVA_{257–264}$-specific $CD8^+$ T cells. Seven days after priming, the magnitude of the $CD8^+$ T cell response was measured by using H-2K^b–OVA tetramers to track $OVA_{257–264}$-specific $CD8^+$ T cell response and by analyzing intracellular IFN-γ expression after restimulation of the Ag-specific $CD8^+$ T cells with the relevant OVA peptide. We observed a 2- to 3-fold decrease in the proportion as well as the absolute number of $OVA_{257–264}$-specific IFN-γ^+ $CD8^+$ T cells at the peak (day 7) of the primary response in *Def6*$^{-/-}$ mice compared with WT mice (Fig. 1A–D). Furthermore, the reduced expansion of *Def6*$^{-/-}$ OVA-specific $CD8^+$ T cells was not due to differential homing or trafficking of the cells, as a similar degree of decrease was observed in all organs tested; namely, the BM, liver, lymph node, blood, and spleen (Fig. 1D, 1E). Taken together, these results suggest that SLAT is required for optimal expansion of Ag-specific $CD8^+$ T cells after in vivo priming.

SLAT is dispensable for $CD8^+$ T cell differentiation into effector CTLs

Next, we assessed the influence of *Def6* deletion on the activation and effector function of $CD8^+$ T cells by analyzing several phenotypic and functional parameters characteristic of effector $CD8^+$ T cells. Expression of the key regulatory transcription factors, T-bet and Eomesodermin (Eomes), shown to control CTL effector programming (22, 23), was similar in WT and *Def6*$^{-/-}$ OVA-specific $CD8^+$ T cells after Ag priming (Fig. 2A). Moreover, analysis of surface expression patterns of KLRG-1 and CD127, which phenotypically discriminate terminally differentiated short-lived effector cells (SLECs; KLRG-1^{high}CD127^{low}) from long-lived memory precursor effector cells (MPECs; KLRG-1^{low} CD127^{high}), showed no difference between responding WT and *Def6*$^{-/-}$ $CD8^+$ T cells (Fig. 2B). Furthermore, *Def6*$^{-/-}$ $CD8^+$ T cells were proficient at effector cytokine production, as similar frequencies of IFN-γ– or IFN-γ/TNF-α–producing $CD8^+$ T cells were found among the responding $CD8^+$ T cells from Act-mOVA–immunized WT and *Def6*$^{-/-}$ mice (Fig. 2C). Finally, despite a defective Ag-induced primary expansion of $CD8^+$ T cells in *Def6*$^{-/-}$ mice, the remaining $CD8^+$ T cells displayed intact in vivo cytolytic activity (Fig. 2D). Altogether, these data suggest that *Def6* deficiency, while impairing the expansion of $CD8^+$ T cells, did not alter either $CD8^+$ T cell differentiation into effector CTLs or the effector function of differentiated CTLs.

Intrinsic effects of Def6 *deficiency on $CD8^+$ T cell expansion*

The defect in *Def6*$^{-/-}$ $CD8^+$ T cell priming could reflect defective activation of $CD4^+$ Th cells or impaired function of Ag-presenting dendritic cells (DCs), which also express SLAT. Therefore, we wanted to determine whether the observed defect is $CD8^+$ T cell–intrinsic. To this end, we crossed *Def6*$^{-/-}$ mice onto an OT-I background, in which the majority of $CD8^+$ T cells express a Vα2Vβ5 TCR recognizing the $OVA_{257–264}$ peptide presented in the context of H-2K^b (24). We adoptively cotransferred equal numbers of naive (CD62L^{high}CD44^{low}) WT CD45.1$^+$ and *Def6*$^{-/-}$ CD45.2$^+$OT-I $CD8^+$ T cells into WT CD45.1/2$^+$ recipient mice. Of note, we transferred a very small number of cells (50 each) to most closely mimic the endogenous $CD8^+$ T cell response without suppressing it (17, 25) (as shown in Fig. 3A, *right column*). The next day, we immunized the recipient mice with Act-mOVA/$K^{b-/-}$ splenocytes and evaluated the expansion of WT and *Def6*$^{-/-}$ $CD8^+$ T cells, which were identified based on their distinct CD45 congenic markers, at the peak of the response (day 7). We observed a substantial clonal expansion of donor WT OT-I cells in the blood (Fig. 3A) and spleen (Fig. 3C) as evidenced by frequency and absolute number of the recipient mice. By contrast, the expansion of *Def6*$^{-/-}$ OT-I T cells was significantly diminished (Fig. 3A, 3C). Calculation of the ratio of WT to *Def6*$^{-/-}$ OT-I cells in the recipient mice showed that WT $CD8^+$ cells expanded on average ~2.5 times more than the *Def6*$^{-/-}$ cells (Fig. 3B). However, the expanded *Def6*$^{-/-}$ OT-I cells displayed a frequency of SLECs and MPECs similar to that of WT OT-I cells (Fig. 3E) and a only small decrease in T-bet and Eomes expression (Fig. 3D) and in IFN-γ/TNF-α–producing cells (Fig. 3F) compared with WT cells. Furthermore, *Def6*$^{-/-}$ and WT donor OT-I T cells displayed similar cytolytic activity in vivo and ex vivo (Supplemental Figs. 1A and 1B, respectively) and $CD8^+$ T cell degranulation determined by cell surface modulation of CD107a/LAMP-1 upon Ag encounter (Supplemental Fig. 1C). Overall, these results recapitulate the data obtained in intact immunized

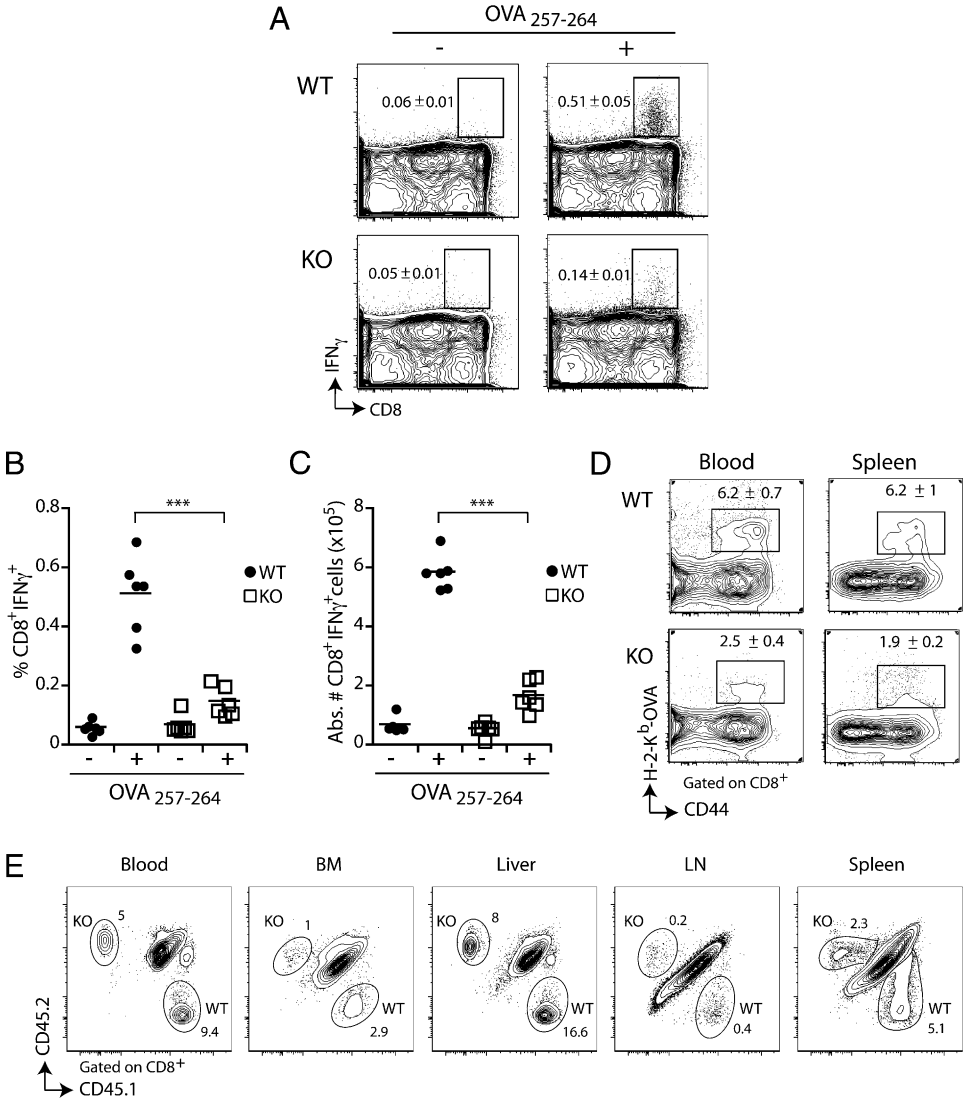

FIGURE 1. *Def6* deficiency results in defective CD8$^+$ T cell primary expansion. (**A**–**D**) Mice were challenged, and Ag-specific CD8$^+$ T cell response in the spleen and blood was assayed 7 d later by IFN-γ ICS after 5 h of ex vivo restimulation in the presence (+) or absence (−) of the OVA$_{257–264}$ peptide (A–C) and OVA$_{257–264}$/K^b tetramer staining (D). Representative FACS plots (A), frequency (B), and absolute number (C) of IFN-γ–producing WT and *Def6*$^{-/-}$ knockout (KO) CD8$^+$ T cells present in the spleen (n = 6 per group) are shown. Numbers shown in the FACS plots are the percentage ± SEM for each group of mice. Dots and squares represent individual mice, and means ± SEM are indicated. ***$p < 0.0005$ (two-tailed unpaired t test). (D) Representative FACS plots of WT and KO Ag-specific CD8$^+$ T cells present in the blood and spleen. Numbers shown in the FACS plots are the percentage ± SEM for each group of mice. (**E**) Five hundred naive WT (CD45.1$^+$) and *Def6*$^{-/-}$ (KO; CD45.2$^+$) OT-I CD8$^+$ T cells (expressing an OVA-specific TCR) were adoptively cotransferred into CD45.1/2$^+$ B6 recipient mice that were immunized 1 d later with 5 × 10^6 Act-mOVA/K$^{b-/-}$ splenocytes followed by flow cytometry analysis at day 7. The frequency of WT and KO OT-I CD8$^+$ T cells among the lymphocytes from the blood, BM, liver, lymph node (LN), and spleen is indicated. Data are representative of five independent experiments.

mice (Figs. 1, 2) and, moreover, clearly indicate that the defect in the priming and expansion of Ag-specific T cells observed in *Def6*$^{-/-}$ mice is CD8$^+$ T cell–intrinsic.

The cross-priming model using Act-mOVA/K$^{b-/-}$ splenocytes as immunogens has been shown to result in accelerated acquisition of memory phenotype and function, and effector CD8$^+$ T cells cross-primed under these conditions respond vigorously to short-interval reexposure to Ag (26). This accelerated memory development is evident from the prevalence of MPECs over SLECs 7 d after Ag priming (Fig. 3B, 3E). We took advantage of this system to examine further the importance of SLAT in the secondary expansion of CD8$^+$ T cells after ActA-deficient (ActA$^-$) Lm-OVA challenge. We observed a drastically diminished (4- to 5-fold) accumulation of *Def6*$^{-/-}$ OT-I CD8$^+$ T cells by comparison with WT cells 5 d after Lm-OVA infection (Supplemental Fig. 2A–C). In contrast, the phenotypic (Supplemental Fig. 2D, 2E) and functional (Supplemental Fig. 2F) parameters of Ag-specific CD8$^+$ T cells were not affected by *Def6* deletion (Supplemental Fig. 2).

We extended this analysis to a different priming model, which does not display the accelerated memory phenotype; namely, priming of mice with Lm-OVA. When CD8$^+$ T cell priming was analyzed 7 d after Lm-OVA immunization, we observed similar results to those obtained in mice primed with Act-mOVA/K$^{b-/-}$ splenocytes; that is, impaired expansion of the *Def6*$^{-/-}$ T cells (Fig. 3G). The delayed development of T cell memory was evident from the finding that on day 7 postpriming, the Ag-specific response as determined was dominated by SLECs (Fig. 3H). As in the case of CD8$^+$ T cells from Act-mOVA/K$^{b-/-}$ splenocyte–primed mice (Supplemental Fig. 2A–C), *Def6*$^{-/-}$ T cells also displayed an impaired secondary T cell expansion after ActA$^-$ Lm-OVA rechallenge at day 54 (Supplemental Fig. 3).

Impaired proliferation and enhanced death of Def6$^{-/-}$ *CD8*$^+$ *T cells*

To investigate further the cause of the reduced expansion of *Def6*$^{-/-}$ CD8$^+$ T cells, we first evaluated their proliferative capacities in vivo. We transferred CFSE-labeled WT or *Def6*$^{-/-}$ CD45.2$^+$ OT-I CD8$^+$ T cells into WT B6.SJL (CD45.1$^+$) mice, immunized the recipients with Act-mOVA/K$^{b-/-}$ splenocytes, and analyzed the accumulation of the donor cells and their division profile by CFSE dilution in recipient spleens. *Def6*$^{-/-}$ CD8$^+$ T cells exhibited impaired accumulation compared with WT cells, reflecting a significantly lower number of cycling cells (Fig. 4A). Analysis of cell number recovered at each division cycle showed that *Def6*$^{-/-}$ CD8$^+$ T cells divided at a rate similar to that of WT cells in response to OVA priming during the first two cycles but displayed a reduced rate at subsequent division cycles (Fig. 4B). This

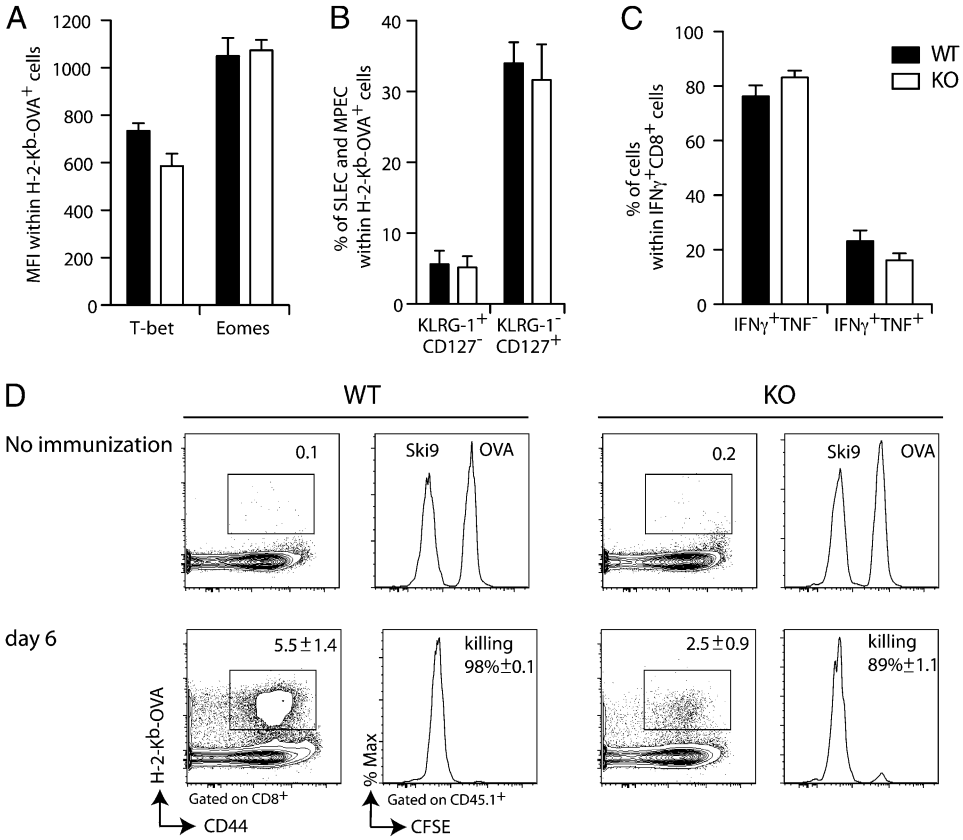

FIGURE 2. SLAT is not required for CD8+ T cell differentiation into primary effector CTLs. Mice were primed with 5×10^6 Act-mOVA/$K^{b-/-}$ splenocytes. On day 7, $OVA_{257–264}$/K^b-specific CD8+ T cells were stained with H-2K^b–OVA tetramer, and IFN-γ– and TNF-α–producing CD8+ T cells were assessed by ICS after restimulation with OVA peptide for 5 h. (**A**) Expression of T-bet and Eomes within the $OVA_{257–264}$/K^b-specific CD8+ T cell population. (**B**) Expression of KLRG1 and CD127 on OVA/K^b-specific CD8+ T cells. KLRG-$1^{high}CD127^{low}$ CD8+ T cells are referred to as SLECs, whereas KLRG-$1^{low}CD127^{high}$ CD8+ T cells are referred to as MPECs. (**C**) Frequency of IFN-γ– and TNF-α–producing CD8+ T cells within the IFN-γ+ CD8+ T cells. Each graph represents the mean of six mice/group and is representative of at least two independent experiments. (**D**) In vivo cytolytic activity of Ag-specific CD8+ T cells from WT versus knockout (KO) mice 6 d after priming with Act-mOVA/$K^{b-/-}$ splenocytes. Data are presented as the frequency of tetramer+ cells (numbers above outlined areas in *first* and *third panels from left*) and killing of target cells pulsed with $OVA_{257–264}$ peptide and loaded with high concentration of the cytosolic dye CFSE (OVA) versus control target cells pulsed with an irrelevant peptide and loaded with a low concentration of CFSE (Ski9) (*second* and *fourth panels from left*). Cytotoxicity was determined 16 h after adoptive transfer of target cells. Numbers in plots indicate percentage ± SEM of specific killing of $CFSE^{high}$, OVA-loaded cells. Data are representative of five independent experiments.

reduced proliferation in response to anti-CD3/CD28 stimulation was confirmed by measuring [^{3}H]thymidine incorporation (Supplemental Fig. 4A). With regard to cell survival, we could not assess the proportion of dying cells in vivo, presumably due to the rapid engulfment of apoptotic cells by phagocytes. However, we determined the frequency of dividing versus dying CD8+ T cells in vitro by CFSE labeling and concurrent staining with active caspase-3 and annexin V mAbs, respectively. We confirmed that *Def6*$^{-/-}$ CD8+ T cells divide at a slower rate than WT cells in response to anti-CD3/CD28 stimulation (Fig. 4C, 4D). This proliferative defect was accompanied by a 2-fold reduction in the proportion of surviving *Def6*$^{-/-}$ CD8+ T cells compared with WT cells at all time points assayed (Fig. 4C, 4E). Consistent with their reduced proliferation along with enhanced cell death, anti-CD3/CD28–stimulated *Def6*$^{-/-}$ CD8+ T cells displayed a drastic decrease in IL-2 production (Supplemental Fig. 4B), although CD3/CD28 engagement induced intact upregulation of CD25 and the activation marker CD69 in *Def6*$^{-/-}$ CD8+ T cells (Supplemental Fig. 4C). Because IL-2 has been shown to be required for survival (but not for the initiation of CD8 T cell cycling) to sustain CD8 T cell primary expansion (27), we assessed whether addition of exogenous IL-2 could rescue the survival and/or the proliferation defect of *Def6*$^{-/-}$ CD8+ T cells. Addition of IL-2 restored *Def6*$^{-/-}$ CD8+ T cell survival at all times assayed (Fig. 4C, 4E) but did not rescue the proliferative defect (Fig. 4C, 4D), indicating that the impaired proliferation of *Def6*$^{-/-}$ CD8+ T cells reflects a cell-intrinsic defect, whereas the in vitro survival defect was a consequence of diminished IL-2 production. These data collectively suggest that in the absence of SLAT, CD8+ T cell cycling is intrinsically reduced and IL-2–dependent survival is decreased, with both of these effects combining to result in a drastic defect in primary CD8+ T cell expansion.

Dependence of Ag-specific CD8+ T cell expansion on SLAT-mediated Cdc42 and NFAT1 activation

Next, we investigated the molecular mechanism underlying SLAT-mediated CD8+ T cell expansion. Because SLAT functions as a TCR-regulated GEF for the Rho GTPase, Cdc42, and this activity is required for subsequent NFAT activation and, consequently, for differentiation of CD4+ T cells into effector Th cells (6), we first determined whether NFAT activation in CD8+ T cells was also dependent on SLAT. TCR/CD28 costimulation of naive WT CD8+ T cells resulted in the rapid (5 min) translocation of NFAT1 from the cytoplasm to the nucleus (28, 29); this translocation was still evident after 2 h (Fig. 5A). In sharp contrast, no NFAT1 nuclear translocation was observed in stimulated *Def6*$^{-/-}$

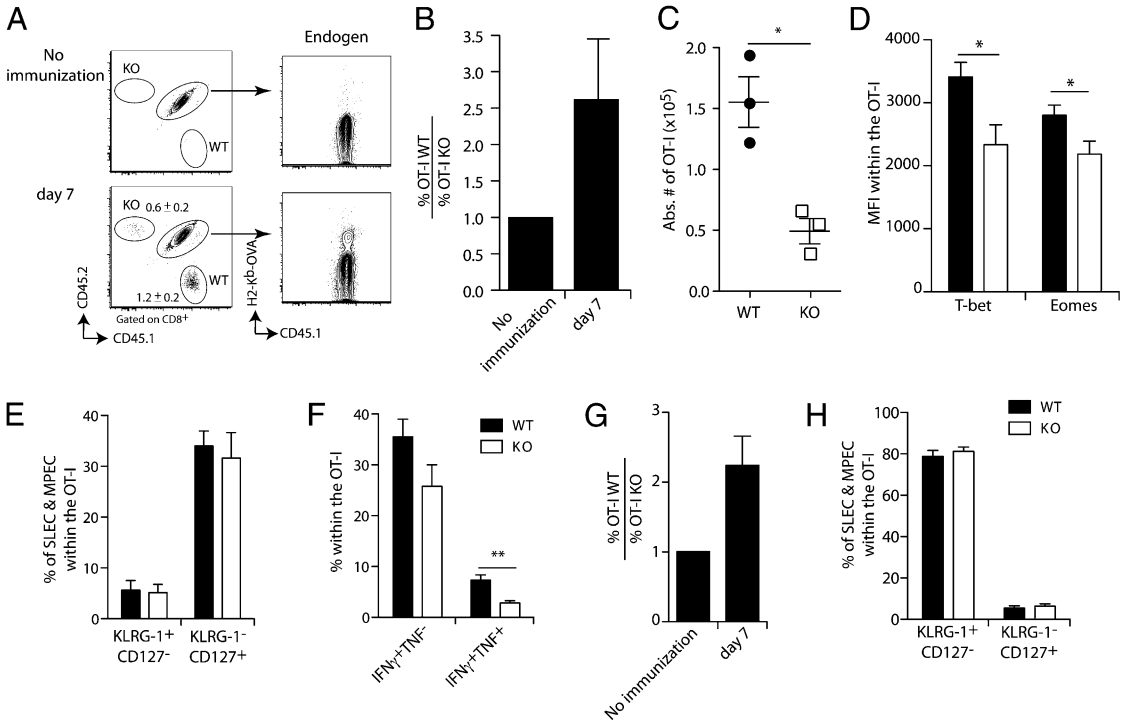

FIGURE 3. SLAT regulates CD8$^+$ T cell expansion in a T cell–intrinsic manner. Fifty naive WT (CD45.1$^+$) OT-I and *Def6*$^{-/-}$ (knockout [KO] CD45.2$^+$) OT-I CD8$^+$ T cells were adoptively cotransferred into CD45.1/2$^+$ B6 recipient mice that were immunized 1 d later with 5 × 10^6 Act-mOVA/K$^{b-/-}$ splenocytes (**A**–**F**) or 1 × 10^7 CFU ActA-deficient, OVA-expressing *L. monocytogenes* (Lm-OVA ActA$^-$) (**G**, **H**) followed by analysis at day 7. (A) Frequency of WT and KO OT-I T cells among the CD8$^+$ T cell population in the blood of a representative mouse (n = 10). (B and G) Average ratio of WT OT-I to KO OT-I CD8$^+$ T cells (n = 10). The WT/KO ratio in nonimmunized animals is set at 1. (**C**) Absolute number of WT and KO OT-I CD8$^+$ T cells among total splenocytes from recipient mice (n = 3). (D) Expression of the KLRG-1 and CD127 on CD45.1$^+$ and CD45.2$^+$ peripheral blood CD8$^+$ cells. (E and H) Mean expression ± SEM of T-bet and Eomes by CD8$^+$ T cells. Data are representative of at least three independent experiments. (F) Frequency of WT and KO OT-I CD8$^+$ T cells producing IFN-γ alone (IFN-γ$^+$TNF-α$^-$) or both IFN-γ and TNF-α (IFN-γ$^+$TNF-α$^+$) among total splenocytes determined by ICS. Data are representative of five (A–F) and three (G, H) independent experiments. *$p < 0.05$, **$p < 0.005$ (two-tailed unpaired t test).

CD8$^+$ T cells (Fig. 5A), indicating that SLAT is required for NFAT1 activation in naive CD8$^+$ T cells as well. This result prompted us further to assess whether constitutively active forms of Cdc42 or NFAT1 can restore the impaired expansion of *Def6*$^{-/-}$ CD8$^+$ T cells in vivo. For this purpose, we used a retrovirus-mediated stem cell gene transfer to generate retrogenic BM chimeric mice, which served as a source of naive CD8$^+$ T cell expressing constitutively active Cdc42 (Cdc42^{CA}) or NFAT1 (NFAT1^{CA}) (Fig. 5B). In the case of NFAT, we used an active mutant that contains two additional point mutations, which prevent NFAT homodimerization (the anergy-inducing form of NFAT) but allow NFAT:AP-1 heterodimerization leading to productive T cell activation (termed hereafter "NFAT1^{CA}Δdimer") (18). This mutant was able constitutively to transactivate an NFAT-responsive reporter luciferase gene in unstimulated T cells (Supplemental Fig. 2G). Sorted GFP$^+$ (transduced) BM stem cells, isolated as Lin$^-$ cells, were transferred into sublethally irradiated *Rag1*$^{-/-}$ recipients, thus allowing the development of donor-derived T lymphocytes in vivo (30). Six to eight weeks after BM transfer, naive (CD62L^{high}CD44^{low}) peripheral blood OT-I CD8$^+$ T cells were sorted, and a 1:1 mixture of 50 each of mock-transduced WT cells and *Def6*$^{-/-}$ CD45.2$^+$ cells transduced with either Cdc42^{CA} or NFAT1^{CA}Δdimer were adoptively transferred into WT CD45.1/2$^+$ recipient mice (Fig. 5B). Seven days after challenge with Act-mOVA splenocytes, we found that the defective *Def6*$^{-/-}$ CD8$^+$ T cell primary expansion was restored when the cells were transduced with Cdc42^{CA} as well as with NFAT1^{CA}Δdimer (Fig. 5C, 5D). Likewise, when rechallenged with Lm-OVA, the *Def6*$^{-/-}$ OT-I CD8$^+$ T cells expressing Cdc42^{CA} or NFAT1^{CA}Δdimer, but not the mock-transduced *Def6*$^{-/-}$ cells, displayed secondary expansion very similar to that of the control, mock-transduced WT cells (Supplemental Fig. 2H, 2I). Together, these findings suggest that defective NFAT signaling, which depends on SLAT-mediated Cdc42 activation, is the cause of the impaired Ag-specific CD8$^+$ T cell expansion.

Discussion

In this study, we investigated the impact of *Def6* deficiency on different phases of Ag-specific CD8$^+$ T cell responses (i.e., activation, expansion, effector function, and memory development). We report that SLAT is a critical CD8$^+$ T cell–intrinsic positive regulator of T cell expansion but is not required for CD8$^+$ T cell differentiation into effector or memory cells. Moreover, we provide evidence that the reduced Ag-induced expansion of CD8$^+$ T cells in the absence of SLAT results primarily from a T cell–intrinsic defective activation and proliferation of clonal precursors, inducing consequently impaired IL-2–dependent cell survival. Lastly, our finding that the expression of constitutively active mutants of Cdc42 or NFAT1 in naive CD8$^+$ T cells rescued the defective Ag-specific CD8$^+$ T cell response suggests that SLAT controls CD8$^+$ T cell expansion through a Cdc42/NFAT pathway.

The CD8$^+$ T cell expansion defect was observed both in a polyclonal environment (i.e., in intact immunized mice) and in a TCR-Tg adoptive transfer system. The results of the adoptive transfer experiments provide evidence that the expansion defect is intrinsic to the Ag-specific CD8$^+$ T cells, although it does not exclude potential contribution by other cell types that also express SLAT such as DCs or CD4$^+$ T cells, which are well known to play

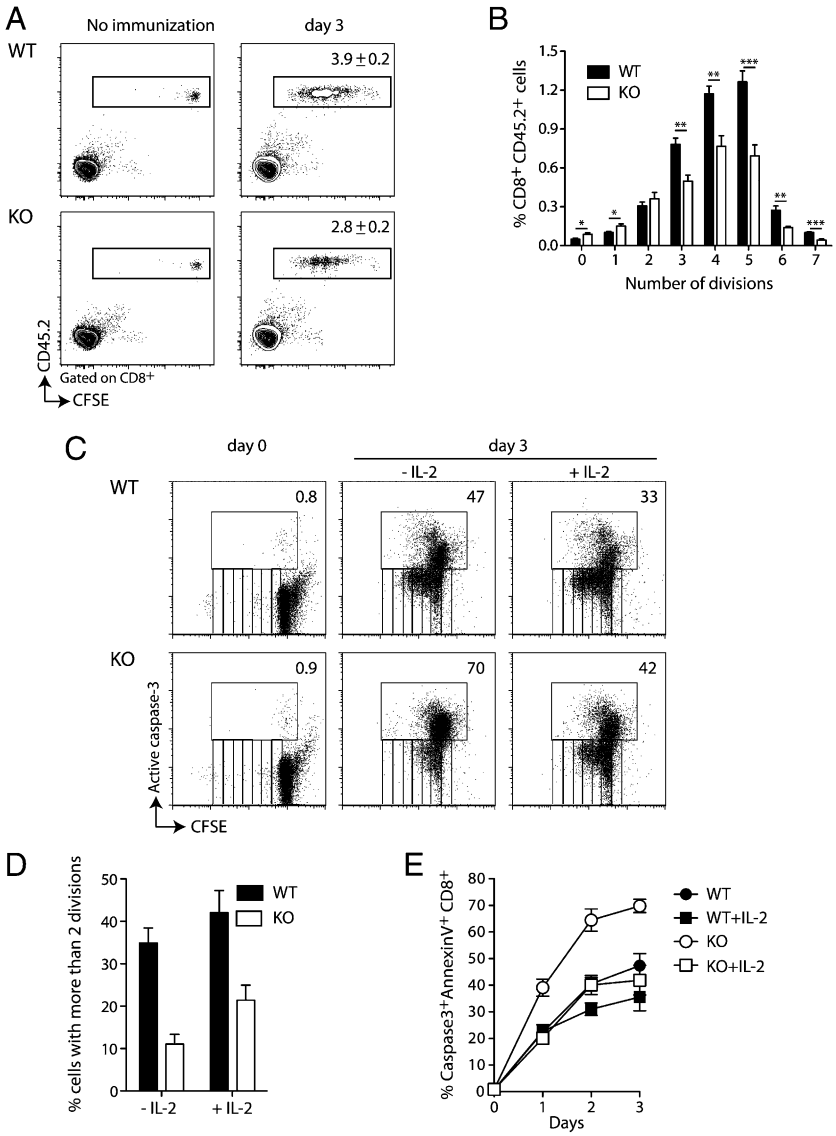

FIGURE 4. SLAT is required for proliferation and IL-2–dependent survival of CD8$^+$ T cells. WT or knockout (KO) (CD45.2$^+$) OT-I CD8$^+$ T cells (5×10^5) were labeled with CFSE and injected i.v. into naive B6.SJL (CD45.1$^+$) mice. One day later, the mice were immunized with 5×10^6 Act-mOVA/K$^{b-/-}$ splenocytes. Splenocytes were harvested 3 d later, and the proliferation of OT-I cells was analyzed by FACS analysis of CFSE dilution after gating on live CD8$^+$ T cells. (**A**) Numbers in the *right panels* indicate the percentage of WT or KO OT-I CD8$^+$ T cells among CD8$^+$ splenocytes (mean ± SEM of six to seven mice). (**B**) Frequency of OT-I cells at each cell division cycle. *$p < 0.05$, **$p < 0.005$, ***$p < 0.0005$ (two-tailed unpaired *t* test). (**C–E**) CFSE-labeled purified CD8$^+$ T cells from WT or *Def6*$^{-/-}$ (KO) mice were stimulated with plate-coated anti-CD3 (5 μg/ml) plus soluble anti-CD28 (2.5 μg/ml) mAbs for 72 h in the presence or absence of exogenous IL-2 (100 U/ml). Cells were then stained with annexin V and active caspase-3 Ab and analyzed by flow cytometry. (C) CFSE dilution and active caspase-3 staining allow concurrent assessment of cell division and cell death of CD8$^+$ T cells. Numbers indicate the percentage of active caspase-3$^+$ cells. (D) The percentage of active caspase-3$^-$ CD8$^+$ T cells with more than two divisions upon 72 h of stimulation is shown. (E) The percentage of active caspase-3$^+$ annexin V$^+$ CD8$^+$ T cells at the indicated times is determined. Data are representative of four (A, B) and three (C–E) independent experiments.

a critical role in the generation of an optimal CD8$^+$ T cell response. However, we have previously shown that *Def6*$^{-/-}$ DCs did not display any defect in Ag presentation to CD4$^+$ T cells (11).

The proliferation of naive CD8$^+$ T cells during a primary response follows a two-phase pattern. The first phase, occurring in the secondary lymphoid organs (SLOs), reflects an initial IL-2–independent expansion of Ag-specific T cells after interaction with APCs. The second phase, which correlates with emigration of the activated CD8$^+$ T cells to peripheral, nonlymphoid target tissues, is associated with the acquisition of effector functions and corresponds to an IL-2–dependent prolonged proliferation of CD8$^+$ T cells within the target organs (27, 31, 32). It is highly likely that SLAT plays a prominent role in CD8$^+$ T proliferation during the early phase of proliferation in SLOs, where the initial Ag-specific T cell–APC interaction occurs. This notion is supported by several findings: First, the expansion defect in *Def6*$^{-/-}$ CD8$^+$ T cells was detected in the spleen. Second, the proliferation defect was observed as early as 3 d postimmunization, when the cells did not yet migrate to the periphery. Third, the acquisition of effector functions and CD8$^+$ T cell survival, associated with the latter stage of the proliferative phase, were not altered in the absence of SLAT. Finally, the impaired proliferation observed in response to anti-CD3/CD28 stimulation was not rescued by addition of exogenous IL-2.

In CD4$^+$ T cells, SLAT has previously been shown to play a key role in TCR-mediated activation and Ag-specific immunological synapse (IS) formation and stabilization at the T cell–APC interface via its actin regulatory function, a process that is critical for optimal T cell activation in SLOs (6, 33). Furthermore, we found that the expression of constitutively active Cdc42, a target of SLAT, rescued the defective expansion of *Def6*$^{-/-}$ CD8$^+$ T cells, demonstrating, for the first time to our knowledge, a role of SLAT and its effector Cdc42 in CD8$^+$ T cell expansion in vivo. On the basis of these observations, and although a role of SLAT in IS formation in CD8$^+$ T cells remains to be formally demonstrated, we hypothesize that altered IS formation, most likely due to abrogated Cdc42-mediated actin accumulation at the T cell–APC interface, accounts for the impaired priming and proliferation of *Def6*$^{-/-}$ CD8$^+$ T cells in vivo. In support of this concept, a recent study showed that SLAT accumulates at the center of the IS, where it may contribute to the activation of Cdc42, which is colocalized at the same site (34). However, several studies ascribe to CDC42 and its effector, Wiskott–Aldrich syndrome protein, a function in later stages of CD8$^+$ T cell differentiation; that is, in

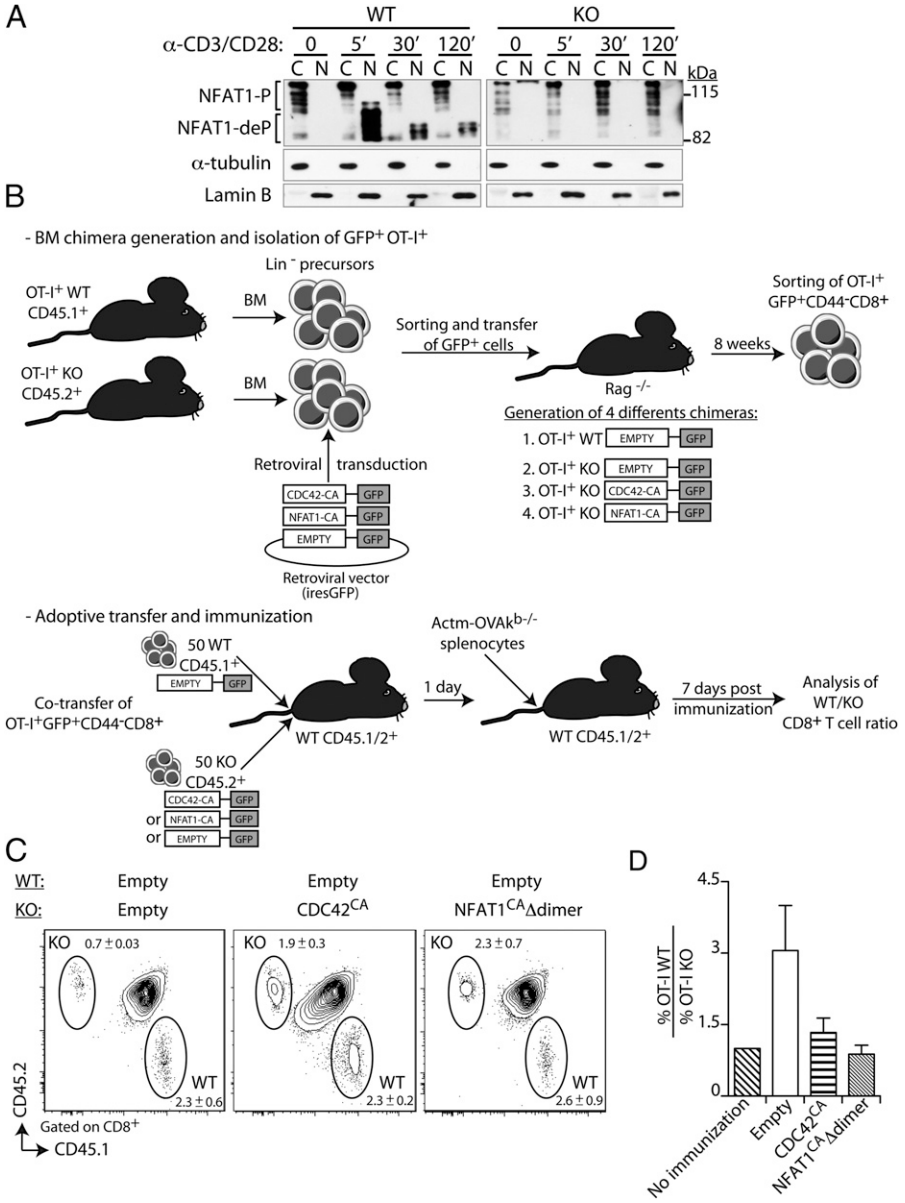

FIGURE 5. Constitutively active Cdc42 or NFAT1 rescue primary expansion of *Def6*$^{-/-}$ CD8$^+$ T cells. (**A**) Primary WT and knockout (KO) CD8$^+$ T cells were activated with anti-CD3 plus anti-CD28 (5 and 2.5 μg/ml, respectively) mAbs for the indicated times. Cytoplasmic (C) and nuclear (N) fractions were immunoblotted with an NFAT1-specific Ab. Fractions were also immunoblotted with α-tubulin– and lamin B–specific Abs to confirm purity of the cytosolic and nuclear fractions, respectively. (**B**) Experimental setup used to assess the role of SLAT-mediated NFAT1 and CDC42 activation in CD8$^+$ T cell expansion. The *top panel* describes the generation of retrogenic mice, followed by sorting of retrovirally transduced (GFP$^+$) naive WT or KO CD8$^+$ T cells, which are used as donor cells for coadoptive transfers into immunized WT recipients, as described in the *bottom panel*. (**C** and **D**) WT (CD45.1$^+$) or KO (CD45.2$^+$) BM progenitor cells from respective OT-I TCR-Tg mice were transduced either with the control empty retrovirus (WT and KO; mock) or with retroviruses encoding the constitutively active Cdc42 (KO; Cdc42^{CA}) or NFAT1 (KO; NFAT1^{CA}Δdimer). Transduced GFP$^+$ BM cells were sorted and injected i.v. into sublethally irradiated *Rag1*$^{-/-}$ mice. Eight weeks later, WT or KO naive OT-I CD8$^+$ cells (tetramer$^+$, CD62L^{high}, and CD44^{low}) were sorted from spleen cell suspensions. WT and KO cells (50 cells each) were transferred as indicated into recipient B6 (CD45.1/2$^+$) mice. One day later, the recipient mice were immunized with 5 × 10^6 Act-mOVA/K$^{b-/-}$ splenocytes and CD8$^+$ T cell expansion of the transferred cells was analyzed on day 7 postchallenge. (C) Frequency of WT and KO OT-I CD8$^+$ T cells among CD8$^+$ T cells in the blood (mean ± SEM, n = 5). (D) Average ratio of WT OT-I to KO OT-I CD8$^+$ T cells (n = 5). The ratio in nonimmunized animals is set at 1. Data are representative of three independent experiments. NFAT1-P, phosphorylated NFAT1; NFAT1-deP, dephosphorylated NFAT1.

the polarization of cytolytic effectors at the CTL–target cell interface, rather than in CD8$^+$ T cell priming (35, 36).

Our data suggest that SLAT functions in CD8$^+$ T cells in a manner distinct from that of other GEFs that are known to activate Cdc42, such as DOCK8 and Vav, as these other GEFs were reported to play a key role in the persistence of CD8$^+$ T cell memory (37) and in CTL lytic activity via regulation of cytolytic effector polarization toward target cells (38, 39). In agreement with the idea that SLAT-mediated CDC42 activation plays a role in CD8$^+$ T cell priming, we have shown that *Def6* deficiency does not impair the formation of effector KLRG1^{hi}CD127^{lo} (SLEC) and memory KLRG1^{lo} CD127^{hi} (MPEC) CTL populations in response to immunization with Lm-OVA or Actm-OVA/K$^{b-/-}$ splenocytes. However, the number of memory cells generated after contraction was reduced, most likely reflecting a secondary outcome of the initial expansion defect. Moreover, a more severe defect in

secondary expansion upon Ag rechallenge was observed (5- to 8-fold reduction in the numbers of *Def6*$^{-/-}$ T cells depending on the immunization model) compared with the 2- to 3-fold defect in T cell expansion after Ag priming (Supplemental Figs. 2, 3). This difference suggests an additional role of SLAT in memory T cell expansion, in addition to its crucial role in primary CD8$^+$ T cell expansion. Supporting a role of Cdc42 in the first phase of CD8$^+$ T cell differentiation from naive into effector cells, a gene expression profile of naive versus effector CD8$^+$ T cells has shown that Cdc42 was upregulated in effector, but not in memory, CD8$^+$ T cells by comparison with naive CD8$^+$ T cells (40). However, in the case of *Def6* deficiency, the cytolytic activity, degranulation, and cytokine production evaluated in equivalent numbers of CTLs from immunized mice was also not altered. Altogether, these observations suggest that SLAT, unlike other Cdc42 activators, may be part of a qualitatively unique TCR-induced signalosome or it may be involved in stage-specific signaling pathways that control CD8$^+$ T cell expansion but not other phases of the response. Of note, these findings held true in several distinct experimental settings, which differ by the strength of the antigenic stimulation and level of inflammation; that is, the splenocyte cross-priming pathway (in the absence of overt systemic inflammation) versus the more inflammatory Lm-OVA model. Consistent with these in vivo findings, *Def6*$^{-/-}$ CD8$^+$ T cells also showed a clear proliferative defect in response to anti-CD3/CD28–mediated costimulation in vitro independently of the concentration of the anti-CD3 Ab (Supplemental Fig. 4A). These findings suggest that SLAT is not critically involved in setting signaling thresholds, but rather it qualitatively modulates TCR signaling.

Primary CTL expansion in vivo is the result of the integration of signals originating from a variety of different signaling cascades, which imprint differentiation of clonal precursors during initial priming into various functional subsets by orchestrating gene programs governed by master transcriptional factors such as STAT1 (41) and Bcl11b (42). Our previous studies in CD4$^+$ T cells show that SLAT is a key component of the Ca^{2+}/NFAT signaling pathway, thereby controlling CD4$^+$ T cell differentiation into effector Th1, Th2, or Th17 subsets (6, 10, 11, 21). Although extensively studied in the context of CD4$^+$ T cell activation and differentiation, the role for NFAT during CD8$^+$ T cell responses has been explored by relatively few studies, and none of these specifically addressed its role in clonal expansion of CD8$^+$ T cells. NFAT1 has been shown to partially regulate IFN-γ production by naive CD8$^+$ T cells (13). In a model of chronic viral infection, silencing of cytokine production has been linked to a selective impairment of NFAT nuclear translocation in CD8$^+$ T cells, whereas cell-directed effector functions, such as degranulation and cytotoxicity, remained intact (15). Finally, the calcineurin/NFAT pathway has been implicated in CD8$^+$ T cell tolerance in vivo (14). Because SLAT controls NFAT activation in a CDC42-dependent manner in CD4$^+$ T cells, and we showed in this study that $Cdc42^{CA}$ rescued the defective expansion of the *Def6*$^{-/-}$ CD8$^+$ T cells, we propose that impaired SLAT-dependent, CDC42-mediated NFAT activation is the underlying mechanism for the impaired expansion of CD8$^+$ T cells. Consistent with such a mechanism, our results show that NFAT1 failed to translocate to the nucleus in stimulated *Def6*$^{-/-}$ CD8$^+$ T cells, and, second, a constitutively active form of NFAT1 bypassed *Def6* deficiency and restored CD8$^+$ T cell expansion. Thus, our findings reveal a heretofore unappreciated role for NFAT1 in CD8$^+$ T cell biology by demonstrating for the first time to our knowledge that SLAT controls the clonal expansion of CD8$^+$ T cells in vivo through a CDC42/NFAT signaling pathway. Our findings differ from another study (13) reporting that *Nfat1*$^{-/-}$ CD8$^+$ T cells show a drastic impairment in IFN-γ production after in vitro anti-CD3 stimulation, which we did not observe in the *Def6*$^{-/-}$ T cells. Thus, the absence of SLAT is likely to lead to more compound alterations in signaling compared with NFAT1 deletion, as SLAT may have additional targets beyond NFAT, including some target(s) that could potentially negatively regulate IFN-γ production and antagonize positive regulation by NFAT. In this scenario, IFN-γ expression would be intact even in the absence of SLAT. Further work aimed at elucidating the molecular pathways through which SLAT links Cdc42 to NFAT activation in cycling CD8$^+$ T cells and identifying SLAT-interacting partners in its regulatory signaling complex may unveil targets for the development of vaccination and therapeutic strategies.

Acknowledgments

We thank Yun-Cai Liu for helpful comments; Ann J. Canonigo-Balancio and Susan Togher for mouse genotyping; and Cheryl Kim, Kurt Van Gunst, and Anthony Jose for assistance with flow cytometry and cell sorting.

Disclosures

The authors have no financial conflicts of interest.

References

1. Sprent, J., A. D. Judge, and X. Zhang. 2002. Cytokines and memory-phenotype CD8+ cells. *Adv. Exp. Med. Biol.* 512: 147–153.
2. Arens, R., and S. P. Schoenberger. 2010. Plasticity in programming of effector and memory CD8 T-cell formation. *Immunol. Rev.* 235: 190–205.
3. Watts, T. H. 2005. TNF/TNFR family members in costimulation of T cell responses. *Annu. Rev. Immunol.* 23: 23–68.
4. Mescher, M. F., J. M. Curtsinger, P. Agarwal, K. A. Casey, M. Gerner, C. D. Hammerbeck, F. Popescu, and Z. Xiao. 2006. Signals required for programming effector and memory development by CD8+ T cells. *Immunol. Rev.* 211: 81–92.
5. Parish, I. A., and S. M. Kaech. 2009. Diversity in CD8(+) T cell differentiation. *Curr. Opin. Immunol.* 21: 291–297.
6. Bécart, S., A. J. Balancio, C. Charvet, S. Feau, C. E. Sedwick, and A. Altman. 2008. Tyrosine-phosphorylation-dependent translocation of the SLAT protein to the immunological synapse is required for NFAT transcription factor activation. *Immunity* 29: 704–719.
7. Tanaka, Y., K. Bi, R. Kitamura, S. Hong, Y. Altman, A. Matsumoto, H. Tabata, S. Lebedeva, P. J. Bushway, and A. Altman. 2003. SWAP-70-like adapter of T cells, an adapter protein that regulates early TCR-initiated signaling in Th2 lineage cells. *Immunity* 18: 403–414.
8. Gupta, S., J. C. Fanzo, C. Hu, D. Cox, S. Y. Jang, A. E. Lee, S. Greenberg, and A. B. Pernis. 2003. T cell receptor engagement leads to the recruitment of IBP, a novel guanine nucleotide exchange factor, to the immunological synapse. *J. Biol. Chem.* 278: 43541–43549.
9. Gupta, S., A. Lee, C. Hu, J. Fanzo, I. Goldberg, G. Cattoretti, and A. B. Pernis. 2003. Molecular cloning of IBP, a SWAP-70 homologous GEF, which is highly expressed in the immune system. *Hum. Immunol.* 64: 389–401.
10. Bécart, S., C. Charvet, A. J. Canonigo Balancio, C. De Trez, Y. Tanaka, W. Duan, C. Ware, M. Croft, and A. Altman. 2007. SLAT regulates Th1 and Th2 inflammatory responses by controlling Ca2+/NFAT signaling. *J. Clin. Invest.* 117: 2164–2175.
11. Canonigo-Balancio, A. J., C. Fos, T. Prod'homme, S. Bécart, and A. Altman. 2009. SLAT/Def6 plays a critical role in the development of Th17 cell-mediated experimental autoimmune encephalomyelitis. *J. Immunol.* 183: 7259–7267.
12. Leung-Theung-Long, S., I. Mondor, M. Guiraud, C. Lamare, V. Nagaleekar, P. E. Paulet, M. Rincon, and S. Guerder. 2009. Impaired NFAT transcriptional activity in antigen-stimulated CD8 T cells linked to defective phosphorylation of NFAT transactivation domain. *J. Immunol.* 182: 6807–6814.
13. Teixeira, L. K., B. P. Fonseca, A. Vieira-de-Abreu, B. A. Barboza, B. K. Robbs, P. T. Bozza, and J. P. Viola. 2005. IFN-gamma production by CD8+ T cells depends on NFAT1 transcription factor and regulates Th differentiation. *J. Immunol.* 175: 5931–5939.
14. Fehr, T., C. L. Lucas, J. Kurtz, T. Onoe, G. Zhao, T. Hogan, C. Vallot, A. Rao, and M. Sykes. 2010. A CD8 T cell-intrinsic role for the calcineurin-NFAT pathway for tolerance induction in vivo. *Blood* 115: 1280–1287.
15. Agnellini, P., P. Wolint, M. Rehr, J. Cahenzli, U. Karrer, and A. Oxenius. 2007. Impaired NFAT nuclear translocation results in split exhaustion of virus-specific CD8+ T cell functions during chronic viral infection. *Proc. Natl. Acad. Sci. USA* 104: 4565–4570.
16. Benedict, C. A., A. Loewendorf, Z. Garcia, B. R. Blazar, and E. M. Janssen. 2008. Dendritic cell programming by cytomegalovirus stunts naive T cell responses via the PD-L1/PD-1 pathway. *J. Immunol.* 180: 4836–4847.
17. Feau, S., R. Arens, S. Togher, and S. P. Schoenberger. 2011. Autocrine IL-2 is required for secondary population expansion of CD8(+) memory T cells. *Nat. Immunol.* 12: 908–913.

18. Soto-Nieves, N., I. Puga, B. T. Abe, S. Bandyopadhyay, I. Baine, A. Rao, and F. Macian. 2009. Transcriptional complexes formed by NFAT dimers regulate the induction of T cell tolerance. *J. Exp. Med.* 206: 867–876.
19. Morita, S., T. Kojima, and T. Kitamura. 2000. Plat-E: an efficient and stable system for transient packaging of retroviruses. *Gene Ther.* 7: 1063–1066.
20. Villalba, M., N. Coudronniere, M. Deckert, E. Teixeiro, P. Mas, and A. Altman. 2000. A novel functional interaction between Vav and PKCtheta is required for TCR-induced T cell activation. *Immunity* 12: 151–160.
21. Bécart, S., and A. Altman. 2009. SWAP-70-like adapter of T cells: a novel Lck-regulated guanine nucleotide exchange factor coordinating actin cytoskeleton reorganization and Ca2+ signaling in T cells. *Immunol. Rev.* 232: 319–333.
22. Sullivan, B. M., A. Juedes, S. J. Szabo, M. von Herrath, and L. H. Glimcher. 2003. Antigen-driven effector CD8 T cell function regulated by T-bet. *Proc. Natl. Acad. Sci. USA* 100: 15818–15823.
23. Pearce, E. L., A. C. Mullen, G. A. Martins, C. M. Krawczyk, A. S. Hutchins, V. P. Zediak, M. Banica, C. B. DiCioccio, D. A. Gross, C. A. Mao, et al. 2003. Control of effector CD8+ T cell function by the transcription factor Eomesodermin. *Science* 302: 1041–1043.
24. Hogquist, K. A., S. C. Jameson, W. R. Heath, J. L. Howard, M. J. Bevan, and F. R. Carbone. 1994. T cell receptor antagonist peptides induce positive selection. *Cell* 76: 17–27.
25. Badovinac, V. P., J. S. Haring, and J. T. Harty. 2007. Initial T cell receptor transgenic cell precursor frequency dictates critical aspects of the CD8(+) T cell response to infection. *Immunity* 26: 827–841.
26. Pham, N. L., L. L. Pewe, C. J. Fleenor, R. A. Langlois, K. L. Legge, V. P. Badovinac, and J. T. Harty. 2010. Exploiting cross-priming to generate protective CD8 T-cell immunity rapidly. *Proc. Natl. Acad. Sci. USA* 107: 12198–12203.
27. D'Souza, W. N., and L. Lefrançois. 2003. IL-2 is not required for the initiation of CD8 T cell cycling but sustains expansion. *J. Immunol.* 171: 5727–5735.
28. Ruff, V. A., and K. L. Leach. 1995. Direct demonstration of NFATp dephosphorylation and nuclear localization in activated HT-2 cells using a specific NFATp polyclonal antibody. *J. Biol. Chem.* 270: 22602–22607.
29. Okamura, H., J. Aramburu, C. García-Rodríguez, J. P. Viola, A. Raghavan, M. Tahiliani, X. Zhang, J. Qin, P. G. Hogan, and A. Rao. 2000. Concerted dephosphorylation of the transcription factor NFAT1 induces a conformational switch that regulates transcriptional activity. *Mol. Cell* 6: 539–550.
30. Nakagawa, R., S. M. Mason, and A. M. Michie. 2006. Determining the role of specific signaling molecules during lymphocyte development in vivo: instant transgenesis. *Nat. Protoc.* 1: 1185–1193.
31. Blattman, J. N., J. M. Grayson, E. J. Wherry, S. M. Kaech, K. A. Smith, and R. Ahmed. 2003. Therapeutic use of IL-2 to enhance antiviral T-cell responses in vivo. *Nat. Med.* 9: 540–547.
32. Kündig, T. M., H. Schorle, M. F. Bachmann, H. Hengartner, R. M. Zinkernagel, and I. Horak. 1993. Immune responses in interleukin-2-deficient mice. *Science* 262: 1059–1061.
33. Fanzo, J. C., W. Yang, S. Y. Jang, S. Gupta, Q. Chen, A. Siddiq, S. Greenberg, and A. B. Pernis. 2006. Loss of IRF-4-binding protein leads to the spontaneous development of systemic autoimmunity. *J. Clin. Invest.* 116: 703–714.
34. Singleton, K. L., M. Gosh, R. D. Dandekar, B. B. Au-Yeung, O. Ksionda, V. L. Tybulewicz, A. Altman, D. J. Fowell, and C. Wülfing. 2011. Itk controls the spatiotemporal organization of T cell activation. *Sci. Signal.* 4: ra66.
35. De Meester, J., R. Calvez, S. Valitutti, and L. Dupré. 2010. The Wiskott-Aldrich syndrome protein regulates CTL cytotoxicity and is required for efficient killing of B cell lymphoma targets. *J. Leukoc. Biol.* 88: 1031–1040.
36. Sinai, P., C. Nguyen, J. D. Schatzle, and C. Wülfing. 2010. Transience in polarization of cytolytic effectors is required for efficient killing and controlled by Cdc42. *Proc. Natl. Acad. Sci. USA* 107: 11912–11917.
37. Randall, K. L., S. S. Chan, C. S. Ma, I. Fung, Y. Mei, M. Yabas, A. Tan, P. D. Arkwright, W. Al Suwairi, S. O. Lugo Reyes, et al. 2011. DOCK8 deficiency impairs CD8 T cell survival and function in humans and mice. *J. Exp. Med.* 208: 2305–2320.
38. Cella, M., K. Fujikawa, I. Tassi, S. Kim, K. Latinis, S. Nishi, W. Yokoyama, M. Colonna, and W. Swat. 2004. Differential requirements for Vav proteins in DAP10- and ITAM-mediated NK cell cytotoxicity. *J. Exp. Med.* 200: 817–823.
39. Billadeau, D. D., K. M. Brumbaugh, C. J. Dick, R. A. Schoon, X. R. Bustelo, and P. J. Leibson. 1998. The Vav-Rac1 pathway in cytotoxic lymphocytes regulates the generation of cell-mediated killing. *J. Exp. Med.* 188: 549–559.
40. Kaech, S. M., S. Hemby, E. Kersh, and R. Ahmed. 2002. Molecular and functional profiling of memory CD8 T cell differentiation. *Cell* 111: 837–851.
41. Quigley, M., X. Huang, and Y. Yang. 2008. STAT1 signaling in CD8 T cells is required for their clonal expansion and memory formation following viral infection in vivo. *J. Immunol.* 180: 2158–2164.
42. Zhang, S., M. Rozell, R. K. Verma, D. I. Albu, D. Califano, J. VanValkenburgh, A. Merchant, J. Rangel-Moreno, T. D. Randall, N. A. Jenkins, et al. 2010. Antigen-specific clonal expansion and cytolytic effector function of CD8+ T lymphocytes depend on the transcription factor Bcl11b. *J. Exp. Med.* 207: 1687–1699.